объединенный
институт
ядерных
исследований
дубна

E9 - 12539

G.Zschornack, G.Müller, G.Musiol

X-RAY DIAGNOSTICS ON COLLECTIVE HEAVY ION ELECTRON RING ACCELERATORS

1979

E9 - 12539

G.Zschornack, G.Müller, G.Musiol

X-RAY DIAGNOSTICS ON COLLECTIVE HEAVY ION ELECTRON RING ACCELERATORS

Submitted to "Nuclear Instruments and Methods"

Щорнак Г., Мюллер Г., Музиоль Г. **E9 - 12539**

Рентгеновская диагностика на коллективном ускорителе тяжелых ионов

Для диагностики пучка на коллективном ускорителе тяжелых ионов ОИЯИ в Дубне разработан диагностический метод для анализа электронно-ионных колец на основе измерения характеристического рентгеновского излучения этих колец. Анализ характеристического рентгеновского излучения позволяет определить степень ионизации ионов в электронном кольце и их распределение по заряду, число электронов и ионов в кольце и собственное электрическое поле кольца. Представлены первые результаты измерений характеристического рентгеновского излучения ионов ксенона, наполненного в электронном кольце.

Работа выполнена в Отделе новых методов ускорения ОИЯИ.

Препринт Объединенного института ядерных исследований. Дубна 1979

Zschornack G., Müller G., Musiol G. **E9 - 12539**

X-Ray Diagnostics on Collective Heavy Ion Electron Ring Accelerators

For beam diagnostics at the collective heavy ion electron ring accelerator at the JINR Dubna a diagnostic method for analysing electron-ion rings for measuring the characteristic X-rays from these rings has been developed. The analysis of the characteristic X-ray radiation allows one to determine the ionization degree of the ions in the electron rings, their charge dispersion, the ion and electron number in the ring and the electric self-fields of the ring. The first results of X-ray measurements for electron rings loaded with xenon have been obtained.

The investigation has been performed at the Department of New Acceleration Methods, JINR.

Preprint of the Joint Institute for Nuclear Research. Dubna 1979

1. INTRODUCTION

For beam diagnostics in the collective heavy ion electron-ring accelerator at the JINR, Dubna, a diagnostic method for analysing electron-ion rings by measuring the characteristic X -rays from these rings is developed. The accurate knowledge of such important parameters as the ionization degree of the ions, the electron and ion number in the ring and the electric eigenfield of the ring is very useful for the design, control and further development of the collective heavy ion electron-ring accelerator. Until now, beam diagnostics at electron-ion rings has been accomplished under using methods based on measurements of electric and magnetic characteristics of electron-ion rings[1,2], and on synchrotron radiation diagnostics, respectively[3]. Realizing X-ray measurements at the collective electron-ring accelerator, we are able to extract simultaneous quantitative conclusions about the ionization degree of the ions and the ion number in the electron ring.

In the present paper in Chapter two we give a short discussion of the possibilities of analysing the X-ray from electron-ion rings. Chapter three gives a description of the computeraided X-ray spectrometer working at the Dubna electron-ring accelerator. Finally, in Chapter four we present first results of measuring the X-ray spectra of xenon ions, stored in the electron-rings of the collective electron-ring accelerator.

2. PHYSICAL FUNDAMENTALS

Crossing the electron-rings, the atoms or ions are ionized by electron-impact ionization of relativistic electrons. Thereby, inner-shell vacancies arise in the atomic electron shells by continuum ionization and following Auger- and Coster-Kronig-processes with outer-shell electron ionization and by second order ionization processes (for in-

stance, double Auger processes, electron-shake-off). The ionization processes occuring after continuum ionization, lead to an acceleration of the ionization course because they are the origin of multi-vacancies or vacancy cascades in the atom or ion.

If inner-shell vacancies are filled up with electrons from higher lying levels, one can observe characteristic X-rays or Auger-electrons. Both the X-ray energy and the energy of the emitted Auger-electrons depend on the concrete electron configuration in the atom or ion and change with the vacancy configuration in the electron electron sub-shells. The vacancy creation is connected with an increased effective potential in which the electrons move themselves because each electron contributes to the shielding of all other electrons from the nucleus potential. The increase of the effective potential leads to a rise in the binding energies of the ion electrons and to a shift of the atomic level energies, which can be measured as a shift of the single X-ray transition energies. The cumulative development of the ionization in the electron-ion rings can be observed by comparing the measured X-ray transition energies with the transition energies of the neutral atom using the results from Dirac-Fock-Slater calculations [4,5]. Such calculations connect the measured X-ray transition energy shifts with fixed degrees of ionization in the atom. In this way, we are not able to observe the creation of outer-shell vacancies in detail, because there appear not or very soft X-rays. However, the information about these ionization states will not be lost, then the energy shift of the next inner-shell X-ray transition contains all information of previous changes in the electron shells of the atom.

Measuring the energy of single X-ray transitions by using a high increasing Ge-detector and converting the analogous information with an analogue-to-digital converter (ADC) in digital form, we added a time mark to each analysed event. The time information corresponds to the time between the beginning of the ion storing time (time from the start of the ion loading in the electron-ring to the acceleration of the electron-ion ring) and the moment of recording the X-ray quantum in the spectrometer. Using this strategy, one can successively analyse single time windows, selecting events, the time information of which lies in the interesting range.

In detail, using the characteristic X-rays from electron-ion rings, one can determine the following quantities:

1. The mean ionization degree from ions in selected time windows.

Analyzing, for instance, the characteristic K_{α_1} X-rays for different time windows, we get small shifts in the K_{α_1}-peak positions which correspond to a change in the X-ray transition energies. After comparing the shifts with earlier computed results from Dirac-Fock-Slater calculations, we are able to obtain conclusions about the development of the mean ionization degree in the electron-ion ring. For instance, we give in Figure 1 the dependence on the energy shifts from some xenon X-ray transitions as a function of the ionization degree of the ion.

2. The ion charge dispersion in the analysed time window.

If the peak area satisfies some statistical limitations[6], we start a procedure to unfold the single X-ray peaks, each of which contains some different components corresponding to different ionization states. Figure 2 shows the statistical boundaries that must be satisfied for unfolding the measured X-ray peaks.

3. The ion number in the electron-ring.

Counting the number of K-events N_K, one can determine the number of ions N_{HI} in the electron-ring by using the formula

$$N_{HI} = \frac{N_K \cdot 2\pi^2 \cdot a^2 \cdot R}{\bar{\sigma}_K \cdot N_e \cdot v_e \cdot t \cdot \omega_K \cdot \epsilon \cdot G \cdot e^{-\mu x}}, \qquad (1)$$

where $\bar{\sigma}_K$ - mean K-shell ionization cross section, N_e - number of electrons, a - radius of the ring cross section, R - radius of the electron-ring, v_e - electron velocity, t - real time of the X-ray measurement, ω_K - K-shell fluorescence yield, ϵ - detector efficiency, G - geometry factor, $e^{-\mu x}$ - intensity losses due to the absorption of the X-rays in the window material and in the air.

For the mean K-shell ionization cross section one can use the cross section for the neutral atom, if a time window is used, by which the mean ionization degree is not greater than ten. By its, based on the Kolbenstvedt model[7], own calculations show that the K-shell ionization cross section for xenon or uranium changes less than 1%.

4. The electron number in the ring.

Filling the compressor chamber with xenon gas under

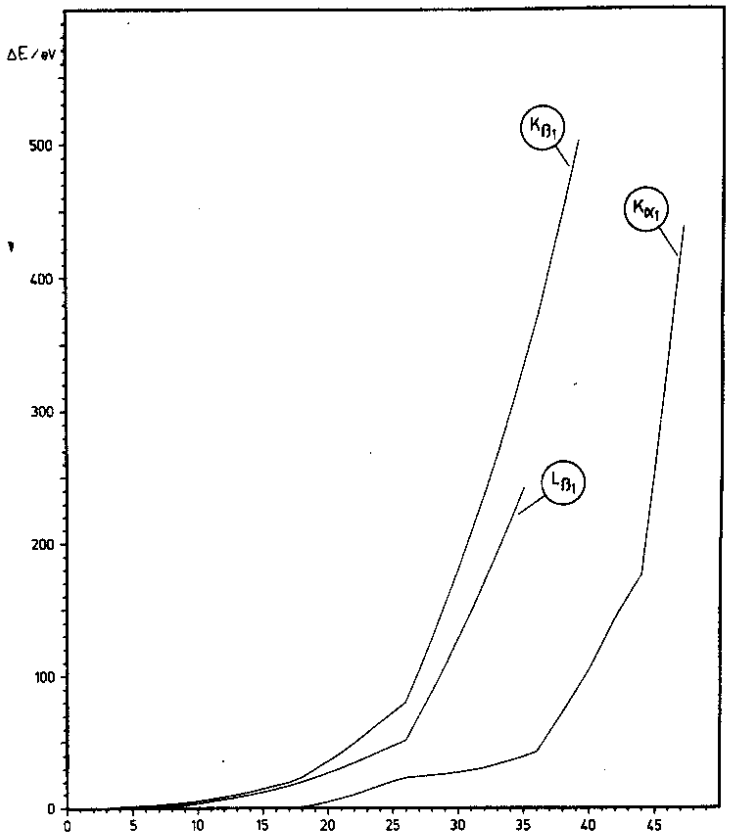

Fig. 1. The dependence of some xenon X -ray transition energies on the ionization degree in the ion.

a well-known pressure, one can calculate the expected X - ray yield, if the ring geometry is known. A certain source of information about the ring geometry at the Dubna electron-ring accelerator is the measurement of the synchrotron light of the ring. The number of electrons can be calculated from the measured X-ray yield N_K:

$$N_e = \frac{N_K \cdot a^2 \cdot R}{1.792 \cdot 10^{15} \cdot \bar{\sigma}_K \cdot v_e \cdot t \cdot \omega_K \cdot \epsilon \cdot G \cdot \xi \cdot e^{-\mu x} \cdot p}, \quad (2)$$

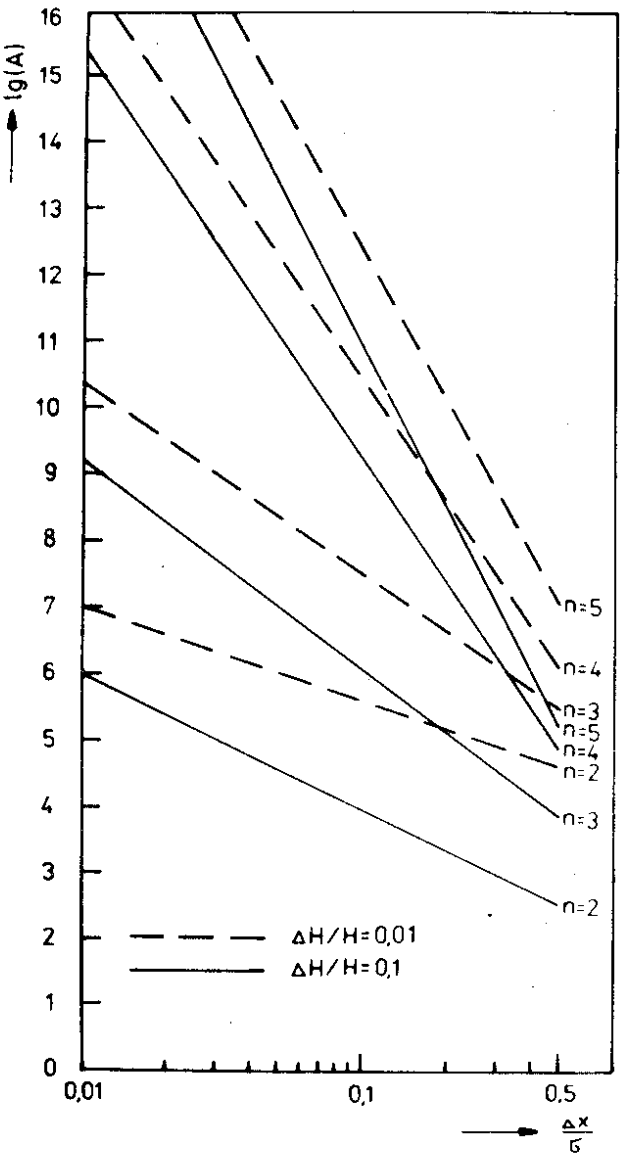

Fig. 2. Statistical boundaries for unfolding measured X - ray sum peaks. A -peak area; Δx - distance of the single peak components; σ - standard variance; $\Delta H/H$-error of the determination of the single peak heights.

where p is the pressure in Torr and ξ is a coefficient, which depends on the ring lifetime and which characterizes the trapping of atoms in the electron-ring by its ionization.

5. Estimation of the electric ring selffield from the X-ray Doppler spreading.

The ions move in the ring so, that the X-rays are emitted by a moving source. Is the motion directed along the axis detector-source, one can observe a Doppler shift of the characteristic X-ray energies, dependent on the velocity of the ions. For the energy spread ΔE becomes, for instance, for a single ionized ion

$$\Delta E = 2E_{K\alpha_1}\left(1 - \frac{v}{c}\cos\theta\cos\rho\right)$$
$$= 2E_{K\alpha_1}\left(1 - \sqrt{\frac{e \cdot N_e}{2\pi\epsilon_0 m c^2 R^2}}\cos\theta\cos\rho\right), \qquad (3)$$

where $E_{K\alpha_1}$ energy of the K_{α_1}-X-rays, ϵ_0 - absolute dielectric constant, e - electric elementar charge, c - velocity of light, m - electron mass.

The electric field in formula (3) is given by $e \cdot N_e / 4\pi\epsilon_0 \cdot R^2$. For the explanation of the angles θ and ρ, look at Figure 3. The factor two in equation (3) originates from the fact that the velocity vector is once directed to the detector and one other time away from it.

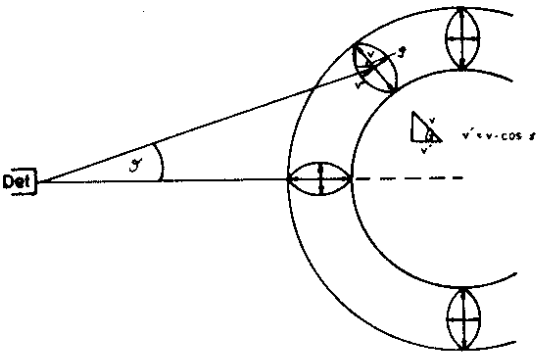

Fig. 3. The measuring geometries for the estimation of the electric ring eigenfield from X-ray Doppler spreading.

The Doppler spreading can be directly observed by the spreading of the full width half maximum (FWHM) of a single X-ray peak since the FWHM of an isolated peak can be described by

$$FWHM = \sqrt{E_{det}^2 + E_{electr}^2 + E_D^2} \quad , \qquad (4)$$

where E_{det} - noise contribution from the detector, E_{electr} - noise contribution from the electronics, E_D - Doppler spreading of the X-ray energy.

It is necessary to note that for the analysis one must choose such a time window in which the X-ray energy shifts, caused from ionization processes, lie in the region of millielectronvolts.

3. THE X-RAY SPECTROMETER

For X-ray measurements on electron-ion rings of the Dubna collective heavy ion electron ring accelerator, a computeraided X-ray spectrometer was developed. The scheme is presented in Figure 4.

To measure the characteristic X-rays, a high purity Germanium detector with a pulsed optical feedback preamplifier is used. The detector is considered in a certain lead shielding in connection with a strong collimator system to avoid overloading processes in the detector system due to the accelerator radiation background. Since the accelerator background also contains fast neutrons from (γ,n)-reactions, we have provided special arrangements to protect the germanium crystal by a combination of a beryllium and a paraffin layer.

The preamplified energetic signal is so amplified in the spectroscopic amplifier that it can be processed by the following electrons. To optimize the energy resolution the amplifier contains an active baseline restorer and Pole/Zero compensation. The preamplified signal simultaneously gets to a pile-up unit which inspects the arriving signals of impulse overlapping. The gaussian shaped energetic signal gets to an impulse stretcher to vary its rise time and width so that the signal would stay ideally compatible with the following ADC. Using the external gate of the impulse stretcher, the signals are always suppressed if the pile-up rejector finds an impulse overlapping or if a feedback cycle occurs in the preamplifier. Moreover, in the pile-up unit all dead

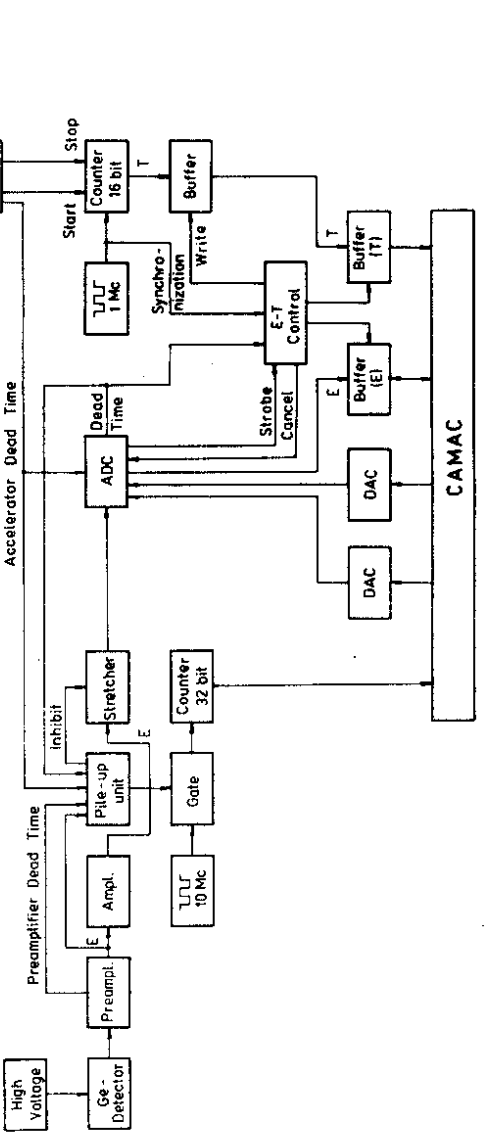

Fig. 4. The scheme of the computeraided X-ray spectrometer.

time signals are summarized to a system dead time signal. This signal gates a counter on which input lies a 10 Mc impulse rate. The counter content can be read by CAMAC and is used to determine the real measuring time.

The stretched and formed energetic signal is digitalized with an ADC which is gated by the accelerator dead time signal. This signal corresponds to the time between the moment of the electron-ion ring acceleration and the recommencement of the ion loading in the next ring. Therefore, the conversion is only allowed for this time when the electron-ion ring contains in the compressor chamber.

To add synchronnely a time mark to each energetic information, a 16 bit synchrotron counter is started to count a 1 Mc impulse rate at the beginning of the gas inlet in the compressor. After starting a conversion in the ADC, the converter generates a dead time signal which serves to trigger an intermediate buffer for registrating the actual content of the synchrotron counter. Ending the conversion, trigger signals for buffering the energy information and the attached time are generated in the control unit. If the buffer capacity is reached, a block transfer in the memory of the minicomputer which writes the energy and time information on magnetic tape for the endprocessing at a great computer, occurs.

To stabilize the X-ray spectrometer against temperature drifts, instabilities of the power supply, changes in the amplification and variations in the counting rate, the position change of selected peaks is analyzed. Basing on the deviation of the peak positions in comparison with the peak positions in the beginning of the experiment, correction values for two digital-to-analogous converters (DAC) are computed by the minicomputer. The corresponding, due to the DAC generated voltages, serve for the correction of the ADC zero threshold and the ADC slope.

4. RESULTS FROM THE FIRST X-RAY MEASUREMENTS ON ELECTRON-ION RINGS

We have accomplished some experiments to measure xenon X-rays at the Dubna collective heavy ion electron-ring accelerator. For simplicity, it is chosen a geometry by which the detector looks through the acceleration tube at the ring plane. By this geometry the X-rays are attenuated by an entrance window of 40 μm titan folie and 135 cm air.

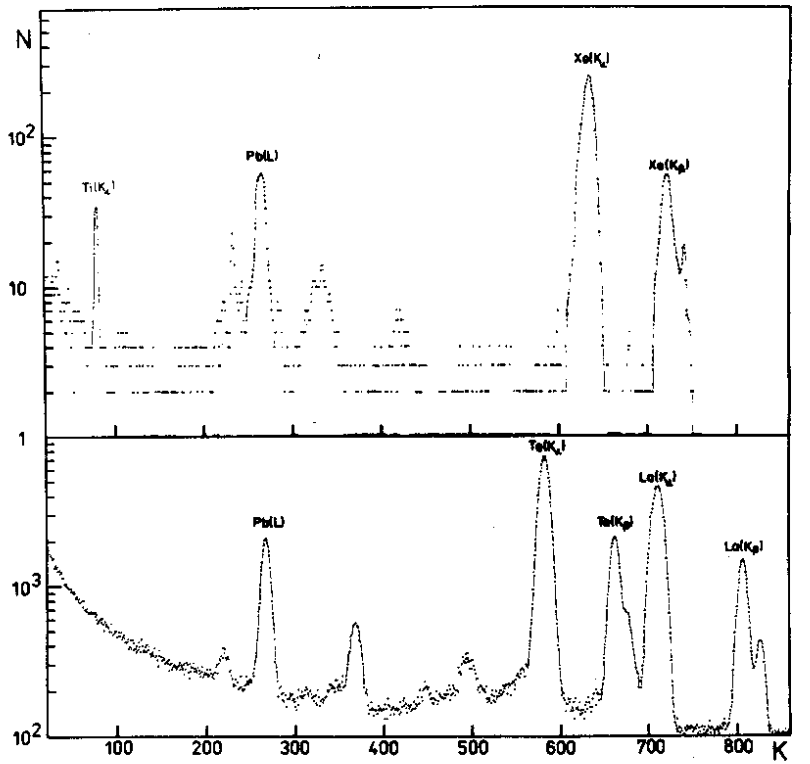

Fig. 5. X-ray spectrum from xenon loaded electron ring. For comparison, a calibration spectrum obtained by fluorescence excitation is shown. The calibration gives approximately 47 eV per channel that corresponds to an energy resolution at the measured titan K-line of 171 eV.

The corresponding attenuation ratios (I/I_0) at 30 keV X-ray energy are $(I/I_0)_{titan} = 0.914$ and $(I/I_0)_{air} = 0.95$, respectively[8]. Using a detector with a volume of 0.7 cm^3 by 7 mm depth, the geometry factor becomes the value of 3.21×10^{-7}.

Figure 5 shows the measured xenon X-ray spectrum from the electron-ion ring. Compared with it, a calibration spectrum from K-shell fluorescence excitation of some elements with a 10 mCi ^{57}Co-source is shown. Besides some characteristic K-X-ray groups, one can recognize the lead L-X-rays from the shielding device. These X-rays also appear by measurements at the accelerator itself because

the electron bremsstrahlung quanta cause fluorescene excitation in the lead of the detector shielding device. As expected, in the measured xenon X-ray spectrum one can also see a peak from titan KX-rays, caused by fluorescence excitation in the titan window, the intensity of which is some orders greater than one of the xenon LX-rays. The real measuring time for the xenon spectrum shown in Fig. 5 was 0.84 sec that corresponds to 700 acceleration cycles with a measurement time of 1.2 msec oer cycle.

In Figure 6 a photograph of some characteristic signals is shown. The low lying positive rectangular pulse corresponds to the measuring time and the mean curve characterizes the course of the guide magnetic field from the coil which performs the final compression of the electron-ring (ring radius 3.5 to 4 cm, radius of the ring cross section 0.3 cm). On upper representation one can see the signal from a scintillation counter which has measured the electron bremsstrahlung by the catching and collection of the xenon ions in the electron-ring. The xenon gas impulse has a length of about 270μsec and is recognized by the relative great amplitude of the output from the electron multiplier (at the abscissa one can consider a time scale of 250μsec per case and at the ordinate the output impulse amplitude with 2.5 V per case). Since the measuring time is essentially fixed after the appearance of the gas impulse, one can conclude that the X-rays at the main point are created by the joint collection of xenon ions in the electron-ring. This fact corroborates the observed electron bremsstrahlung. The bremsstrahlung shows an approximate equal intensity up to the maximum of the magnetic field after which the intensity falls with the decreasing magnetic guide

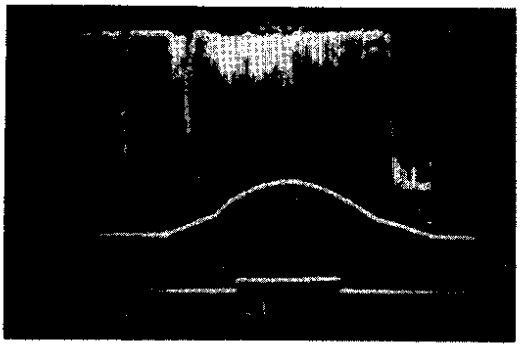

Fig. 6. Photograph of some signals characterizing the collective loading of the electron-ring with xenon ions.

field. During the fall of the magnetic field the electron-ring radius increases, i.e., the electron density decreases. At the end, the great impulse occurs if the electrons fall after the compression on the chamber walls and produce electron bremsstrahlung.

Calculating the product $N_e N_{HI}$ after formula (1) one can get with $\bar{\sigma}_K = 5 \cdot 10^{-23}$ cm^2, $v_e = 0.999$ c, $\omega_K = 0.9$ and ϵ (30 keV) = 0.84 an integral particle number of $(2 \pm 0.82) \cdot 10^{23}$ particles per electron-ion ring. In the described experiments in the compressor chamber the rest gas pressure was of $(5.5\text{-}8) \cdot 10^{-8}$ Torr and the maximum partial xenon pressure in the atomic beam pulse was approximately of $3 \cdot 10^{-6}$. Torr.

First of all, the object of our investigations was to measure the characteristic xenon X-rays from the electron-ion ring and not to get quantitative results about the particle number in the ring. Hence, for exactly quantitative results it is especially necessary to control the coincidence between the injection time of the atomic beam pulse and the electron-ring, which should be at this time crossing the pulse trajectory.

5. CONCLUDING REMARKS

The accomplished experiments show the possibility of performing X-ray measurements with a view to beam diagnostics investigations. Moreover, the excellent signal-to-noise ratio and the sharp energetic resolution seem to be possible to use the electron-ion rings as spectroscopic sources for highly stripped ions. If an atom of the neutral gas has suffered from an ionizing collision, the ion remains trapped in the potential wall of the ring and becomes the target for successive ionizing collisions so that it acquires a progressively higher charge state. In this process the non-relativistic atomic electrons released are expelled by the ring potential and are not available for recombination.

It is necessary to note, that it's essentially no experimental information about the cross sections for collisional ionization of the multiply-charged ions, the change of X-ray intensities and other atomic quantities with varying degree of ionization. The expected results are of fundamental interest in atomic physics. They are also of great importance in astrophysical applications, ion source diagnostics and more recently, in fusion research for the diagnostics of

very heavy ions that can cool plasma in the reactor.

In future, one can hope to obtain X-ray spectra with some order higher statistics so that it would be possible to determine the ion charge dispersion in the ring and further, to get some certain information about the processes which occur in the ion shells during ionization.

6. ACKHOWLEDGEMENTS

The authors would like to thank professor V.P.Sarantsev and Dr. V.A.Sviridov for several stimulating discussions and for the constant interest in our work. We also wish to thank Mr. A.P.Sumbaev for his help in the preparation of the photograph (Figure 6) and Mr. S.I.Tjutjunikov for providing electron bremsstrahlung measurements, which results are shown in the upper part of fig. 6.

REFERENCES

1. Kirjushin J.T., Kolesnikov J.M. JINR, 9-9546, Dubna, 1976.
2. Aleksandrov V.S. et al. JINR, P9-8753, Dubna, 1975.
3. Maltsev A.A. JINR, 13-9663, Dubna, 1976.
4. Siebert H.U. et al. JINR, P9-9657, Dubna, 1976.
5. Zschornack G. et al. JINR, P7-11876, Dubna, 1978.
6. Müller G. et al. JINR, E7-12219, Dubna, 1979.
7. Kolbenstvedt H. Journ. Appl. Phys., 1967, 38, p.4785.
8. With mass attenuation coefficients from Veigele M.J. Atomic Data Tables, 1973, 5, p.51.

Received by Publishing Department
on June 12 1979.